RSC Advances

PAPER

View Article Online
View Journal | View Issue

Cite this: *RSC Adv.*, 2023, **13**, 31128

Gemini ionic liquid-based surfactants: efficient synthesis, surface activity, and use as inducers for the fabrication of Cu_2O nanoparticles†

Kyrillos Roshdy,‡ Hany I. Mohamed, ‡* Mohamed H. Ahmed, Wagdy I. El-Dougdoug and Mohamed A. Abo-Riya *

Received 11th July 2023
Accepted 16th October 2023

DOI: 10.1039/d3ra04646j

rsc.li/rsc-advances

Discovery of green and novel synthetic routes for nanoparticles (NPs) has drawn a lot of interest due to the distinct nano size and unusual features as well as applications of such particles. Ionic liquid-based surfactants (ILBSs) and gemini ionic liquid-based surfactants (GILBSs) have become some of the best choices to be used as inducers or dispersing agents for the fabrication of nanoparticles. This work involves the synthesis, spectroscopic characterization, and surface property evaluation of three novel GILBSs (**4a–c**), which incorporate the imidazolium cation as the polar head with an ethylene spacer. The simple synthetic route includes, first, alkylating imidazole-N1 with the as-prepared fatty alkyl chloroacetates followed by quaternization of two equivalents of imidazole-N2 with ethylene dibromide. Investigations into the compounds' surface characteristics and thermodynamic parameters were carried out. The prepared GILBSs, **4a–c**, were then used as inducers at various concentrations for the preparation of cuprous oxide nanoparticles. The size and shape of the produced NPs were examined by X-ray diffraction (XRD) and transmission electron microscopy (TEM) analysis in each case to study the effect of concentration on the NP morphology and to determine the best concentration for the NPs fabrication. The XRD patterns of the produced Cu_2O NPs contain distinguishable peaks, which refer to crystalline Cu_2O. Also, TEM images show that the obtained Cu_2O is present in form of well dispersed nanorod particles with sizes about 55 and 23 nm at concentrations of 60 and 200 ppm, respectively.

1 Introduction

Ionic liquids (ILs) are salts with low melting points[1] or exist as liquids at room temperature; the latter is known as room temperature ionic liquids (RTILs). Liquids are typically composed of neutral molecules, whereas RTILs are composed of ions.[2,3] Surfactants are amphiphilic compounds composed of molecules with a hydrophobic (non-polar) tail and a hydrophilic (polar) head.[4] Therefore, conventional ILs can be designed to act as surfactants by attaching long hydrophobic chains to their polar heads and are thus referred to as surface active ionic liquids (SAILs) or ionic liquid-based surfactants (ILBSs).[5–25]

Recently, ILBSs have piqued the interest of researchers as promising replacements for conventional surfactants in order to overcome limitations and disadvantages such as high toxicity, non-biodegradability, and the need for a high concentration to form stable micelles. This is due to the promising properties of ILBSs that include high thermal stability, low vapor pressure, non-flammability, low toxicity, biodegradability, and non-volatility.[1,26–28] Furthermore, they are custom-made and highly tunable, allowing them to have good surface activity in both aqueous and emulsion systems,[26,29,30] and to be task-specific.

In the 1930s, a new class of surfactants, gemini surfactants, was discovered and has been found to possess more surface activity than the corresponding conventional surfactants with the same hydrophobic chain and the same hydrophilic head but in a single structure.[31] Similarly, two ILBS units are linked together by a rigid or flexible spacer to form gemini ionic liquid-based surfactants (GILBSs). This can be easily exploited to produce various ILBSs and GILBSs with better physicochemical properties,[15,32–35] allowing them to be utilized in a myriad of applications.

These compounds are used as solvents, as they can dissolve a broad range of inorganic, organic, and polymeric materials. In addition, they are utilized in solar cells, lubricants, separation applications,[36,37] water treatment,[38] drug delivery,[39] as improvers for the enzymatic degradation of textile dyes,[40] corrosion inhibitors,[41] biocatalysts, and as inducers for nanoparticles (NPs) synthesis.[42–46] A stabilizing material that acts as a capping or dispersing agent is required during the synthesis of NPs to prevent the re-accumulation of the particles. Currently, ILBSs

Chemistry Department, Faculty of Science, Benha University, Benha 13518, Egypt. E-mail: mohamed.aborya@fsc.bu.edu.eg; hany.ibrahim@fsc.bu.edu.eg

† Electronic supplementary information (ESI) available. See DOI: https://doi.org/10.1039/d3ra04646j

‡ These authors are equally contributed to the work.

have been used instead of conventional surfactants in the synthesis of NPs as they exhibit better dispersing properties, which make the control of NPs' shape possible. These compounds can be used not only as capping agents but also in the synthesis process.[46]

When ILBSs are used as stabilizers, they help detect the shape and size of NPs by acting as templates for the NPs. These templates are easily customizable to achieve the desired shape and size. Some of the factors that influence the size and shape of the NPs include the length of the hydrophobic chain and the type and number of the ionic groups in ILBSs.[43,47–52] ILBSs with 8 or fewer carbon atoms in their hydrophobic chain lack the effective protection power to stabilize nanoparticles, so the particles tend to accumulate in the moment they are synthesized.[44]

In this work, three new gemini ionic liquid-based surfactants, including imidazolium cation as the polar head and ethane-1,2-diyl as a spacer, were synthesized and characterized. The surface properties and thermodynamic parameters of these compounds were extensively investigated. One of the prepared surfactants was then used at different concentrations in the preparation of cuprous oxide nanoparticles, and the size and shape of the nanoparticles were detected by XRD and TEM in each case to detect the effect of concentration on the morphology of the produced nanoparticles and to detect the best concentration between them in the production of nanoparticles.

2 Experimental section

Materials and instruments

1-Decanol, 1-dodecanol, 1-hexadecanol, 1,2-dibromoethane, copper sulfate pentahydrate and chloroacetic acid were obtained from Sigma-Aldrich. Potassium sodium tartarate tetrahydrate were obtained from Fisher Scientific UK. Imidazole and *p*-toluenesulphonic acid were obtained from Loba Chemie. Glucose, petroleum ether and diethyl ether were obtained from Oxford Lab Fine Chem. Xylene, absolute ethanol, anhydrous sodium sulfate, ethyl acetate and sodium hydroxide were obtained from AL-Nasr chemical company. FT-IR (ATR or KBr disc) were performed on Nicolet iS10 FT-IR spectrophotometer. ^{1}H NMR spectra were generated with Bruker Avance (III) 400 MHz signal (Switzerland), using deuterated dimethyl sulfoxide (DMSO-d_6) or deuterated chloroform ($CDCl_3$) as a solvent and tetramethylsilane (TMS) as internal reference. Surface tension and interfacial tension values were measured by using a De-Noüy ring tensiometer (Kruss-K6). Miniflex 600 Rigaku XRD Instrument was used to confirm the structure of the nanoparticles and detect their sizes. The morphology of nanoparticles was determined by loading the sample on carbon coated copper grid, the grid with the sample on it was then investigated by HR-TEM (JEOL, JEM-2100, Tokyo, Japan). DLS measurements were performed at room temperature (25 ± 2 °C), with a Zetasizer Nano ZS (Malvern Instruments) equipped with a He–Ne laser (k = 633 nm) and a backscatter detector at a fixed angle of 173°.

Synthesis

General procedure for the synthesis of fatty alkyl 2-chloroacetates (2a–c). These derivatives were synthesized as reported previously.[53] Typically, the corresponding fatty alcohol (**1a–c**, 1 equiv.) namely, 1-decanol, 1-dodecanol, or 1-hexadecanol, was added separately to chloroacetic acid (1 equiv.) in dry xylene. The reaction was catalyzed by *p*-toluenesulphonic acid (PTSA, 1 mol%) then the mixture was equipped by Dean–Stark under reflux with stirring at about 170 °C till the formation of one equivalent of water. The produced fatty alkyl 2-chloro-acetates **2a–c** were isolated by extraction with petroleum ether, the organic phases were dried over anhydrous Na_2SO_4, and the solvent was evaporated to dryness *in vaccou*.

*Decyl 2-chloroacetate (**2a**).* Colorless viscous liquid, yield = 74%. FT-IR (ATR) ν/cm^{-1} 2958, 2924, 2854 (C–H of aliphatic fatty chain), 1740 (C=O of ester), 1308, 1172 (C–O), 1288, 790 (C–Cl), (Fig. S1†).

*Dodecyl 2-chloroacetate (**2b**).* Off-white semisolid, yield = 69%. FT-IR (ATR) ν/cm^{-1} 2952, 2923, 2853 (C–H of aliphatic fatty chain), 1736 (C=O of ester), 1308, 1170 (C–O), 1288, 791 (C–Cl), (Fig. S2†).

General procedure for the synthesis of fatty alkyl 2-(1*H*-imidazol-1-yl) acetates (3a–c).[54] Sodium (1 equiv.) was dissolved in a suitable amount of absolute ethanol, then imidazole (1 equiv.) was added. The mixture was stirred at room temperature till the completion of the reaction that had been monitored by TLC. The excess of solvent was evaporated, and the produced white powder (sodium imidazole) was collected. To a solution of sodium imidazole (1 equiv.) in ethyl acetate, chloroacetates (**2a–c**, 1 equiv.), diluted with the same solvent, were separately added. The mixture was heated under reflux with stirring at 80 °C for about 12 h and then extracted with ethyl acetate. The products were obtained after evaporating the solvent from the dried organic phases.

*Decyl 2-(1H-imidazol-1-yl)acetate (**3a**).* Yellow oil, yield = 83%. FT-IR (KBr disc) ν/cm^{-1} 3123 (C–H of imidazole), 2926, 2854 (C–H of aliphatic fatty chain), 1747 (C=O of ester), 1626 (C=N of imidazole), 1073 (C–O). ^{1}H NMR (400 MHz, $CDCl_3$) δ 7.76 (s, 1H, imidazole), 7.08 (s, 1H, imidazole), 6.97 (s, 1H, imidazole), 4.75 (s, 2H, N–**CH$_2$**), 4.14 (t, J = 6.8 Hz, 2H, O–**CH$_2$**), 1.71–1.56 (m, 2H, **CH$_2$**), 1.38–1.20 (m, 14H, **7CH$_2$**), 0.84 (t, J = 6.8 Hz, 3H, **CH$_3$**), (Fig. S3†).

General procedure for the synthesis of GILBSs (4a–c). 1,2-Dibromoethane (0.5 equiv.) was added to a solution of 1-substituted imidazole (**3a–c**, 1 equiv.) in ethyl acetate. The mixture was stirred at 70 °C for long time (≈90 h), then the products were obtained in pure form by evaporating the ethyl acetate and washing the residues several times by diethyl ether.

*3,3′-(Ethane-1,2-diyl)bis(1-(2-(decyloxy)-2-oxoethyl)-1H-imidazol-3-ium) bromide (**4a**).* Colorless viscous liquid, yield = 63%. FT-IR (ATR) ν/cm^{-1} 3418 (OH, hygroscopic water), 3137 (C–H of imidazole), 2958, 2920, 2850 (C–H, aliphatic fatty chain), 1747 (C=O of ester), 1624 (C=N of imidazole), 1183 (C–O). ^{1}H NMR (400 MHz, DMSO-d_6) δ 9.18 (s, 2H), 7.79 (s, 4H), 5.34 (s, 4H), 4.15 (t, J = 6.5 Hz, 4H), 3.36 (t, J = 6.5 Hz, 4H), 1.70–1.50 (m, 4H), 1.43–1.12 (m, 28H), 0.86 (t, J = 6.8 Hz, 6H). GC-EIMS for

$C_{32}H_{56}Br_2N_4O_4$, RT (min) = 24.82 with molecular weight higher than 700.

*3,3′-(Ethane-1,2-diyl)bis(1-(2-(dodecyloxy)-2-oxoethyl)-1H-imidazol-3-ium) bromide (**4b**).* White solid, m. p. = 96–98 °C, yield = 59%. FT-IR (ATR) ν/cm^{-1} 3417 (OH, hygroscopic water), 3111 (C–H of imidazole), 2958, 2921, 2851 (C–H, aliphatic fatty chain), 1750 (C=O of ester), 1627 (C=N of imidazole), 1180 (C–O). ^{1}H NMR (400 MHz, DMSO-d_6) δ 9.17 (s, 2H), 7.79 (d, J = 3.0 Hz, 4H), 5.34 (s, 4H), 4.14 (t, J = 6.6 Hz, 4H), 3.38–3.15 (m, 4H), 1.70–1.52 (m, 4H), 1.52–1.19 (m, 36H), 0.85 (t, J = 6.8 Hz, 6H). GC-EIMS for $C_{36}H_{64}Br_2N_4O_4$, RT (min) = 26.78 with molecular weight higher than 700.

*3,3′-(Ethane-1,2-diyl)bis(1-(2-(hexadecyloxy)-2-oxoethyl)-1H-imidazol-3-ium) bromide (**4c**).* Off-white solid, m. p. = 128–130 °C, yield = 67%. FT-IR (ATR) ν/cm^{-1} 3405 (OH, hygroscopic water), 3109 (C–H of imidazole), 2956, 2918, 2849 (C–H, aliphatic fatty chain), 1751 (C=O of ester), 1624 (C=N of imidazole), 1181 (C–O). ^{1}H NMR (400 MHz, DMSO-d_6) δ 9.12 (s, 2H), 7.78 (d, J = 3.5, 4H), 5.32 (s, 2H), 5.09 (s, 2H), 4.13 (t, J = 6.7 Hz, 4H), 3.36 (t, J = 6.4 Hz, 4H), 1.60 (m, 2H), 1.27 (m, 52H), 0.85 (t, J = 6.8 Hz, 6H). GC-EIMS for $C_{44}H_{80}Br_2N_4O_4$, RT (min) = 35.79 with molecular weight higher than 800.

Surface properties

(a) Surface and interfacial tension measurements. The surface tension (ST) was measured using a Krüss (Model K 6) tensiometer with a platinum ring.[51] Using distilled water and a ST of 72 dyne cm^{-1} at 25 °C, a 0.1% weight surfactant solution was created. Before use, the platinum ring was cleaned with acetone and water. At least three times were required to set the ST value before the average was approved. For the ionic liquid solution-oil system, interfacial tension (IT) was measured at 25 °C using the same ionic liquid solution. The IT value at which the ring broke apart at the interface between the water and oil is identified. The combined IT value of the used paraffin oil and distilled water is 56.2 dyne per cm^{-1}.[53–55]

(b) Foam height. In a 500 mL graduated cylinder set at 25 °C, 100 mL of an ionic liquid aqueous solution at 0.1% (wt) was violently shaken for about 20 seconds. The height of the created foam at the instant the shaking stopped was measured in millimeters (mm).[53,55]

(c) Emulsion stability. A 25 mL graduated cylinder containing 10 mL of a 0.1% (wt) aqueous solution of the ionic liquid and 5 mL of paraffin oil was vigorously shaken for approximately two minutes at 25 °C. The time it took to separate 9 mL of a pure aqueous solution of the ionic liquid from the emulsion system with the cylinder in a steady state was noted as a measure of the emulsion stability.[56,57]

Preparation of cuprous oxide NPs

Fehling's solutions were prepared as follows: Fehling A was prepared by dissolving 3.45 g of $CuSO_4 \cdot 5H_2O$ in 500 mL of distilled water. Fehling B was prepared by dissolving 17.3 g of potassium sodium tartarate tetrahydrate and 6.0 g sodium hydroxide in 500 mL of distilled water.

50 mL of different concentrations (60, 200, and 400 ppm) of **4b** was prepared. For compounds **4a** and **4c**, only 200 ppm were prepared.

(5 mL) of each of (FA) and (FB) were mixed in a beaker and (50 mL) of the prepared concentration of **4a**, **4b** or **4c** was added to the mixture and stirred for (15 min). Then an aqueous solution of (0.5 g) glucose in (5 mL) distilled water was added to the previous mixture and the whole content was then heated at about (60 °C) under continuous vigorous stirring. After about (15–20 min.) of the reaction time a brick-red precipitate of Cu_2O was formed, the precipitate was then filtered off, washed several times by deionized water then with ethanol and it was dried in an oven at (60 °C) for 4 h. The produced cuprous oxide nanoparticles were investigated by XRD and TEM to determine the particle size in each case and comparing the effect of different concentrations on the produced nanoparticles' sizes.

3 Results and discussion

Synthesis

Cationic gemini surfactants showed potent behavior in inhibiting corrosion of metals, controlling sulfate-reducing bacteria and synthesis of nanoparticles.[58–60] Ionic liquid-based surfactants and especially gemini ionic liquid-based surfactants (GILBSs) are promising compounds due to their advanced properties and variable applications. A series of new GILBSs were synthesized according to the following steps (Scheme 1). Firstly, fatty alcohols (1-decanol, 1-dodecanol, 1-hexadecanol) were esterified with chloroacetic acid to produce the corresponding chloroacetates (**2a–c**). FT-IR spectra of these acetates showed characteristic absorption band for carbonyl-ester at around 1750 cm^{-1} beside bands for C–O and C–Cl at 1180 and 790 cm^{-1}, respectively, (Fig. S1 and S2†). Then, these esters were reacted with the as-prepared sodium imidazole to give 1-alkyl imidazole derivatives (**3a–c**). New peaks in FT-IR spectra at around 3100 and 1620 cm^{-1}, which confirm the presence of aromatic C–H and C=N bonds of imidazole, respectively. In addition, their ^{1}H NMR spectra exhibited three signals of aromatic protons at 7–8 ppm, (Fig. S3†).

Finally, the targeted GILBSs **4a–c** were obtained *via* gentle reflux of alkyl imidazoles with 1,2-dibromoethane. In addition to the signals of aromatic and fatty chain protons, new signals appeared in the ^{1}H NMR spectra of GILBSs **4a–c** at around 5.2–5.4 ppm attributable to ethylene spacer protons as clearly shown in Fig. 1, S4, and S5.†

Surface properties

Surface-active attributes measurements of the synthetic ionic liquid (GILBSs) were performed to assess their surface activity, and the resulting data are shown in Table 1.

Surface and interfacial tension

From Table 1, it is clear that by adding GILBSs compounds, the surface tension of water decreases, as well as the interfacial tension, proving that these compounds have the ability to affect the surface tension and work in the interfaces. The table also

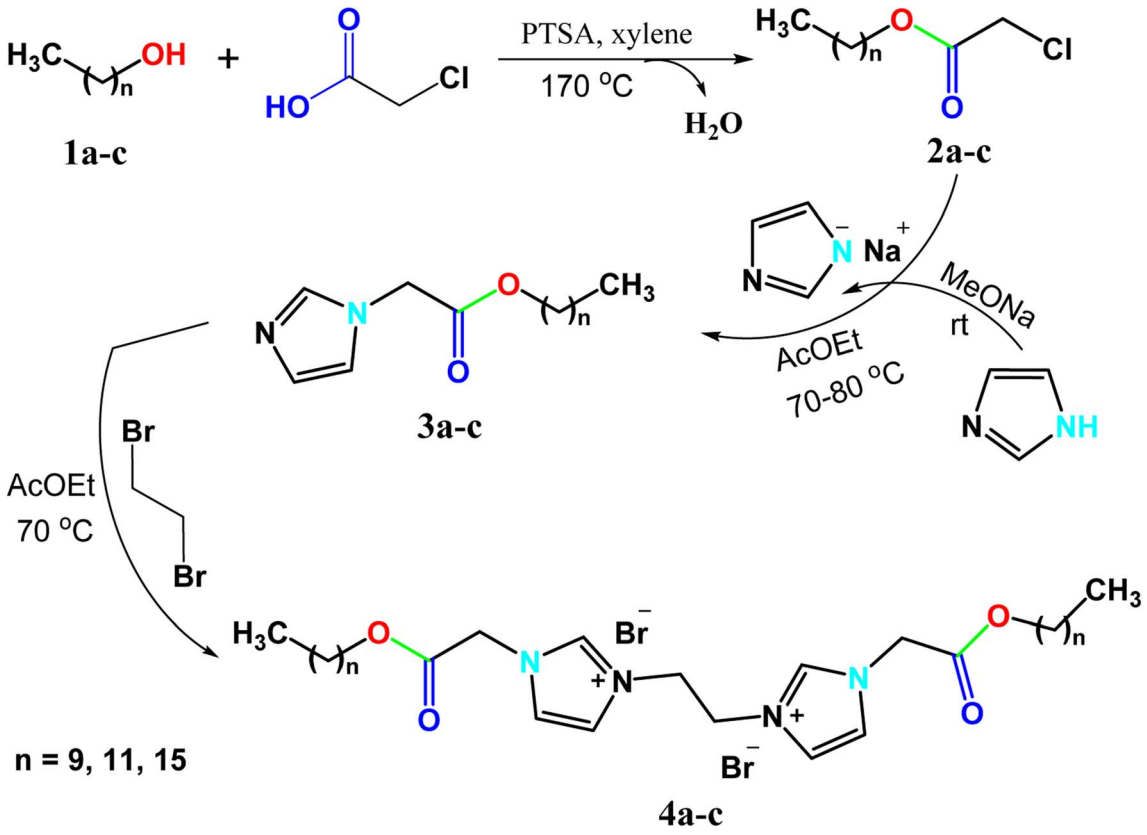

Scheme 1 Synthetic pathway for the targeted GILBSs **4a–c**.

shows that the surface tension rises as the hydrocarbon chain lengthens, suggesting that the compounds' influence on surface tension reduces as the lengthening of the hydrocarbon chain.

Emulsion stability (ES)

The higher the emulsion stability capacity of these compounds, the longer it takes to separate the emulsion. It is evident from Table 1 that the synthetic ionic liquids (GILBSs) have a significant capacity for emulsion formation; however, when hydrophobicity increases, this capacity for emulsion formation decreases, especially with compound **4c**.

Foam height (FH)

The types of applications of GILBSs depend on their capacity to foam and the height of their foam, which is a significant occurrence. All of the prepared GILBSs had a high foaming height, as shown by the data in Table 1. Additionally, the values of foam height often decrease as the length of the fatty chain rises.

Critical micelle concentration (CMC)

Due to the hydrophobic group that these compounds contain, when they are dissolved in water, the molecules start to rise to the water's surface, which helps to lower surface tension. This effect lasts until the molecules stop rising, regardless of how much the concentration of the dissolved substances rises. This occurs as a result of water molecules forming micelles around themselves. This concentration is known as the CMC. Utilizing the surface tension method, it is determined. It was determined by plotting the aqueous GILBSs solutions' corresponding logarithms of concentration and surface tension (Fig. 2). The information is displayed in Table 1, which demonstrates that the CMC values of compounds **4a** and **4b** decrease as the size of the hydrophobic group increases but increase once more in compound **4c**. This might be the fact that **4c** has a huge size makes mobility more challenging, and it hardly ever migrates to the surface.

Effectiveness (π_{CMC})

The calculation of π_{CMC} is used to find out how these compounds can alter the water's surface. The higher the value of π_{CMC}, the greater the compound's capacity to lower the surface tension of water. It was determined using the formula given below using the difference between the surface tension of pure water (γ_o) and the surface tension of the surfactant's aqueous solution at CMC (γ_{CMC}).[61] Results from the π_{CMC} calculations GILBSs are shown in Table 2.

$$(\pi_{CMC} = \gamma_o - \gamma_{CMC}) \quad (1)$$

Maximum surface excess (Γ_{max})

Γ_{max} calculations are made in order to determine the material particle concentration on the water's surface. The amount of ionic liquid particles on the surface has an impact on the

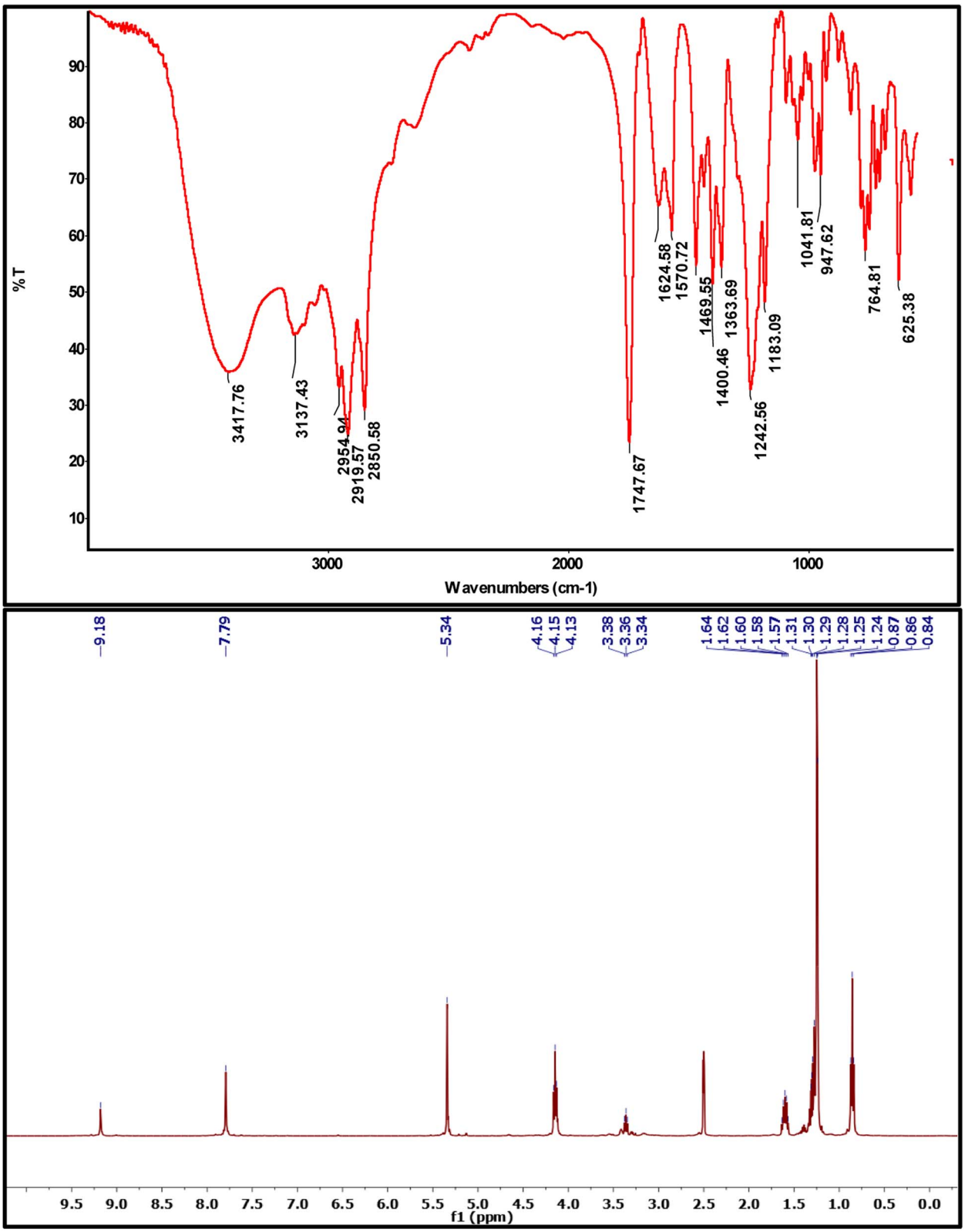

Fig. 1 FT-IR and ^{1}H NMR (DMSO-d_6) spectra for the GILBS **4a**.

water's surface tension, as the greater the number of particles on the surface of the water, the lower the surface tension of the water. Γ_{max} was determined using the Gibbs adsorption isotherm eqn (2).[62]

$$\Gamma_{max} = -(\delta\gamma/\delta \log c)_T/2.303nRT \quad (2)$$

where, $(\delta\gamma/\delta \log c)$ is the slope of the straight-line portion in the surface tension *vs.* −log concentration at 25 °C, $n = 2$ in case of

Table 1 Surface properties of the synthesized GILBSs **4a–c**

GILBS	Surface tension (mN m^{-1})	Interfacial tension (mN m^{-1})	Foam height 0.1% (mm)	Emulsion stability (min:sec)	CMC/mM
4a	35.03	13	140	34:35	2.4
4b	40.77	16.3	120	28:14	2.2
4c	46.07	17.3	110	14:26	3.1

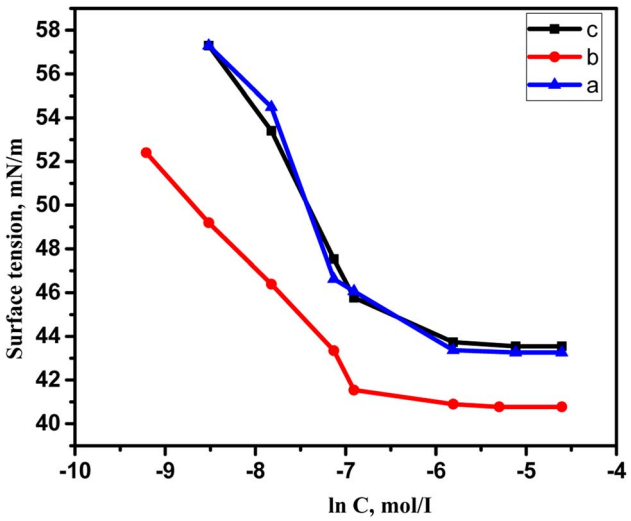

Fig. 2 Variation of surface tension *vs.* the concentration of the synthesized cationic gemini surfactant at 25 °C.

conventional surfactants, R is the gas constant, T is the absolute temperature. Table 2 shows that the concentration of molecules at the air/water interface falls as the hydrocarbon chain lengthens in compounds **4a** and **4b** before increasing once more in compound **4c**.

Minimum surface area (A_{min})

The average surface area occupied by a molecule at the air/water interface is known as A_{min}, eqn (3) has been used to calculate A_{min}.[63]

$$A_{min} = 10^{16}/N_A\Gamma_{max} \quad (3)$$

where A_{min} is in nm^2 and N_A, is Avogadro's constant (6.022×10^{23} mol^{-1}). The space available for each molecule at the air/water contact shrinks as its population grows. According to the findings in Table 2, the A_{min} increases in compound **4a** and **4b** as the number of molecules on the surface decreases.

Thermodynamic parameters of the synthesized ionic liquid

The most crucial characteristics of ionic liquid to be researched are their thermodynamic properties, specifically their adsorption free energy (ΔG°_{ads}) and micellization free energy (ΔG°_{mic}). Through its calculations, we can judge whether the compounds prefer to work inside the solution and form a micelle or migrate to the intersurface. Gibbs adsorption equations (eqn (4) and (5)) were used to calculate micellization and adsorption free energy.[64]

$$\Delta G^{\circ}_{mic} = 2.303RT \log \mathrm{CMC} \quad (4)$$

$$\Delta G^{\circ}_{ads} = \Delta G^{\circ}_{mic} - (0.06023\pi_{cmc}A_{min}) \quad (5)$$

Table 2 displays the values of ΔG°_{mic} and ΔG°_{ads}, which came from eqn (4) and (5). The outcomes show that the micellization and adsorption of Gibbs free energies are both negative. According to fundamental thermodynamic principles, all of the molecules of the ionic liquid being studied tend to spontaneously form micelles in the solution or become adsorbed at the interface.

It is also obvious that the values are more negative than those of, indicating a higher capacity for absorption at the air/water interface than micellization into the solution. From Table 2, it is evident that the ionic liquid compounds have a better probability of being absorbed at the interface as the length of the hydrocarbon chain increases, as opposed to micellization into the solution, as in the case of compounds **4a** and **4b**. This interpretation holds true for compound **4c**, however due to the length of its chain, which makes it harder for it to move, it require a larger energy to have either micellization or adsorption on the interface.

Preparation and characterization of Cu_2O NPs aided by GILBSs

Cuprous oxide stands out as an important oxide due to its several functions. Solar cell,[65] catalysis,[66] and batteries[67] are a few examples of how cuprous oxide is used in chemistry. Many ways have been developed to synthesize Cu_2O NPs such as

Table 2 Thermodynamic parameters of the synthesized GILBSs **4a–c**

Compd	CMC/mM	γ_{CMC}/mN m^{-1}	Π_{CMC}/mN m^{-1}	$\Gamma_{max} \times 10^{11}$/mol cm^{-2}	A_{min}/nm^2	ΔG°_{mic}/kJ mol^{-1}	ΔG°_{ads}/kJ mol^{-1}
4a	2.4	43.62	28.38	5.05	3.2	−14.86	−20.30
4b	2.2	40.89	31.11	3.61	4.6	−15.11	−23.69
4c	3.1	43.37	28.63	5.29	3.15	−14.36	−19.77

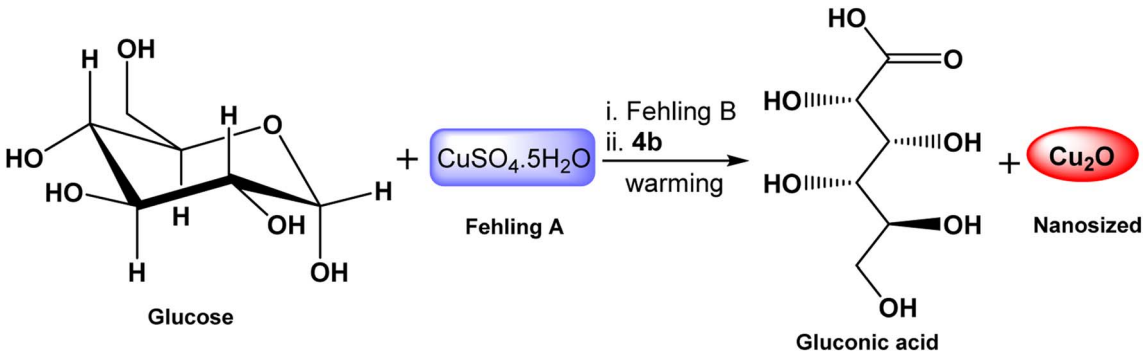

Scheme 2 Preparation route for the Cu_2O NPs induced by GILBS **4b**.

solution-phase,[68] thermal decomposition,[69] and sonication[70] methods. The surfactant-assisted approach is a quick, convenient, and inexpensive way to create size-controllable nanocrystals. Surfactant molecules may work as regulators for the growth of particles or inhibitors for their agglomeration. To prevent the newly formed particles from aggregating, a covering film is formed on top of them.[71,72]

In this work, we used different concentrations of the synthesized GILBS **4b** (60, 200, and 400 ppm) as inducer for the facile preparation of Cu_2O NPs. The conversion of Cu^{2+} to Cu^{+} is brought about by heating Fehling's solution in the presence of a weak reducing agent, like glucose. An orange to red precipitate of Cu_2O is formed as a result of the reduction because the tartarate ion cannot coordinate with the cuprous ion. Actually, when the cupric ion in the tartarate complex comes into touch with the aldehyde group of the glucose molecule, it is reduced to a cuprous ion, and the aldehyde is oxidized to carboxylic acid (Scheme 2). Therefore, we developed a simple technique for the production of Cu_2O NPs employing the GILBS **4b** as surfactants to control the size of these particles by utilizing Fehling's solution's reactivity with glucose.

The transmission electron microscopy (TEM) images of the obtained Cu_2O showed well dispersed roughly nanorod particles (Fig. 3). The mean sizes of Cu_2O nanorods are about 55 nm and 23 nm for the GILBS **4b** at 60 and 200 ppm, respectively. The size of nanoparticles obtained from the TEM studies are in close agreement with those calculated from XRD diffraction patterns.

Patterns for powder XRD for the nanosized Cu_2O were given in Fig. 4 which contain five clearly distinguishable peaks. They are all precisely indexed to crystalline Cu_2O both in terms of peak position and relative intensity. The crystal planes 110, 111, 200, 220, 311 and 222 of crystalline Cu_2O are represented by the peaks with 2θ values of 29.601, 36.521, 42.441, 61.541, 73.691 and 77.611, respectively. The absence of distinctive Cu–O or Cu metal peaks in the XRD patterns suggests that phase-pure cuprous oxide can be produced easily.

Nanowires of Cu_2O with diameter of about 100 nm and lengths of about 16 μm have been prepared by potentiostatic deposition by reduction of alkaline cupric lactate solution at the cathode on polycarbonate membrane. Limitations of this method includes scalability issues, pH management, and accurate temperature control.[73] Firmansyah, *et al.* reported the effect of ethanol on the preparation of Cu_2O NPs by copper nitrate spray pyrolysis. The produced NPs changed, by addition of ethanol, from shell-like to solid-spherical, and their sizes decreased with increasing ethanol volume to 50 nm. This process has some drawbacks, including high temperature, expensive costs, and careful temperature control.[74]

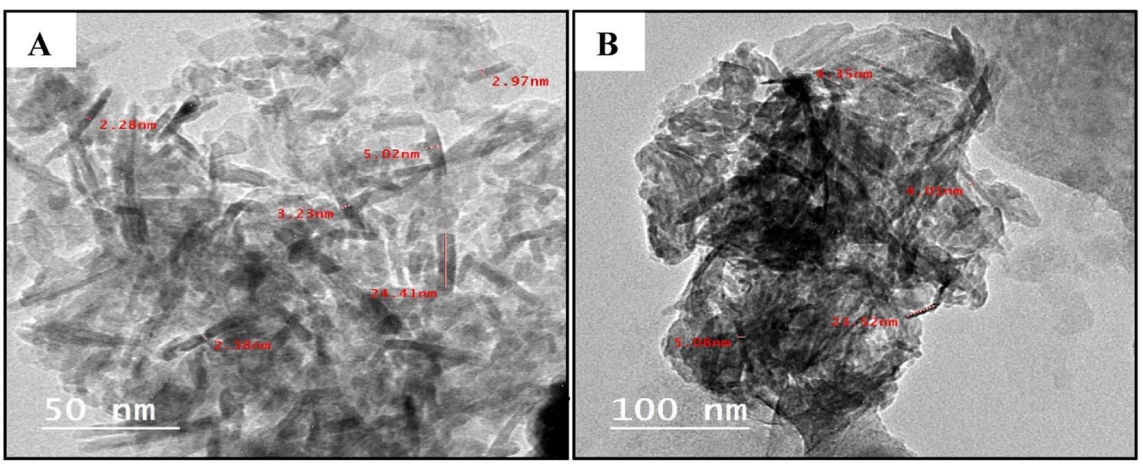

Fig. 3 TEM images of the prepared Cu_2O NPs induced by GILBS **4b** at a concentration of (A) 60 ppm, and (B) 200 ppm.

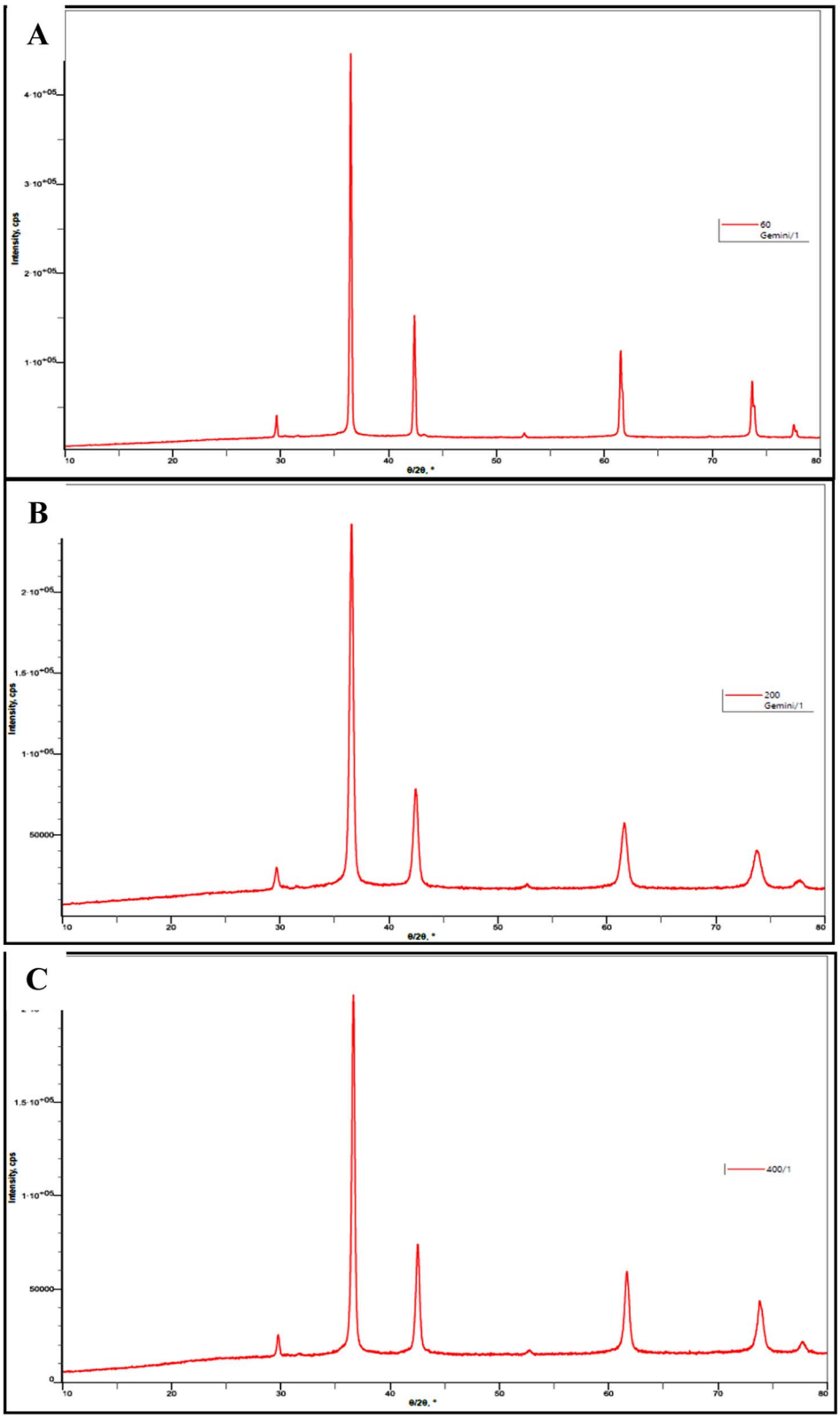

Fig. 4 Powder XRD patterns of the prepared Cu_2O NPs induced by **4b** at (A) 60 ppm, (B) 200 ppm, and (C) 400 ppm.

Furthermore, Cu_2O NPs were synthesized by reduction of copper(II) sulfate present in an aqueous solution containing polyvinylpyrrolidone (PVP), sodium citrate and sodium carbonate, then exposing the produced solution to air for 16 days. The formed NPs have truncated octahedral inner hollow shape with size about 700 nm and inner edge length about

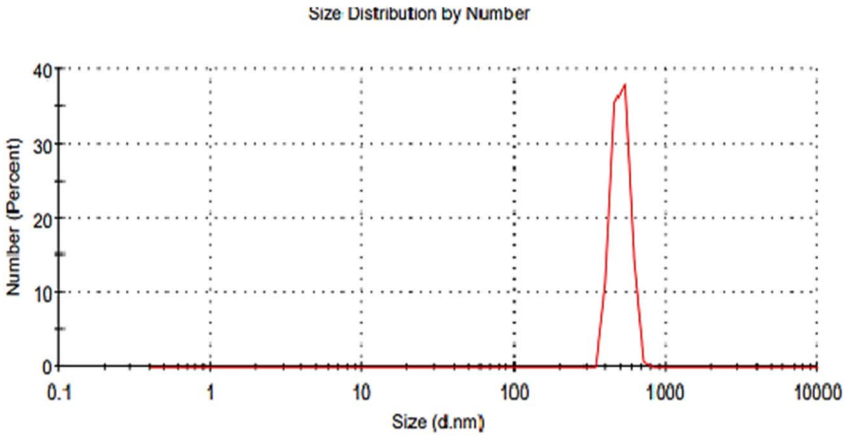

Fig. 5 DLS analysis of the prepared Cu_2O NPs induced by GILBS **4b** at a concentration of 200 ppm.

300 nm. Time-consuming procedure and relatively large particle size limit the application of this method.[75]

For further clarification, nanoparticles formed by using the GILBS **4b** at 200 ppm were examined using Dynamic Light Scattering (DLS) technique. Fig. 5 illustrates that the prepared nanoparticles have an average hydrodynamic diameter of ~531 nm and polydispersity index of 0.796. These results indicate some aggregates formation in the applied dispersant media (water). Furthermore, the crystallite estimated from the XRD results are in good agreement with the TEM results, whereas the size values obtained with DLS are larger. This is due to the fact that the DLS technique measures the hydrodynamic size of the particles. This finding indicates the presence of the solvation layer around the synthesized nanoparticles. However, detailed analysis of the solvation shell is not a subject of this study.

Depending on the previous results, after studying the effect of compound **4b** on the process of Cu_2O NPs preparation, 200 ppm is the most effective concentration in the process of Cu_2O NPs preparation. As a result, experiments were conducted for the other synthesized GILBS **4a** and **4c** at the same concentration.

TEM images of the obtained Cu_2O showed well-dispersed roughly spherical particles and the mean particle sizes of Cu_2O are about 18 nm using compound GILBS **4c**, whereas those prepared using GILBS **4a** are complete and incomplete spherical shape with high agglomeration and not well dispersed with particle size 61.5 nm (Fig. 6).

By comparing the results obtained based on the hydrocarbon chain length, it is evident that the process of Cu_2O NPs preparation is as follows: 61.5 nm, 23 nm, and 18 nm by using GILBS **4a**, **4b** and **4c** at 200 ppm, respectively, which indicates that by increasing the hydrocarbon chain length, these compounds are more effective in forming nanoparticles. This could be because GILBS molecules are more repellent to one another as chain length increases, which helps the molecules spread apart.

XRD data in agreement with those obtained from TEM, with all the peaks related to cuprous oxide and absence of distinctive Cu–O or Cu metal peaks, as in case of **4b**, that can be evidenced on phase-pure of prepared NPs (Fig. 7).

Bai group prepared Cu_2O nanoparticles with different shapes and sizes by reduction of aqueous solution of copper(II) acetate by ascorbic acid, the solution contained NaOH and PVP as a stabilizer. They managed this by changing the concentrations of the different reagents and heating temperature.[76] Similarly, Huang and Chiu synthesized Cu_2O NPs by redox reaction from copper chloride in presence of NaOH, hydroxyl amine and SDS as an inducer. The particle size ranges from 40 to 420 nm.[77] Our strategy utilizes a novel synthesized GILBSs as inducers for the fabrication of nano-sized cuprous oxide. It could overcome almost all the limitations of the previously reported methods as it does not need pH management, high

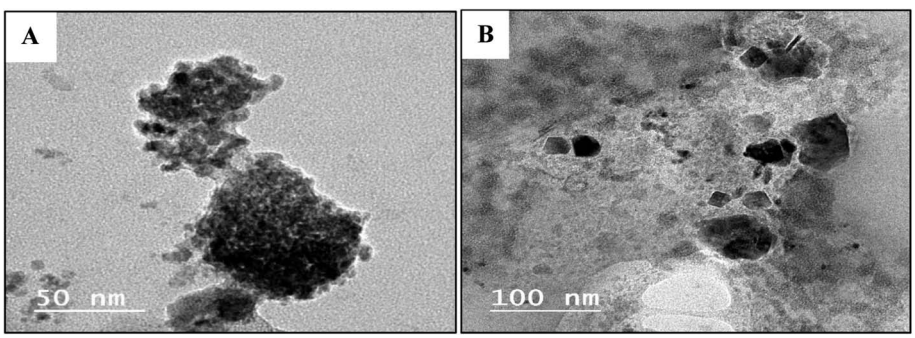

Fig. 6 TEM images of the prepared Cu_2O NPs induced by GILBS **4a** (A) and **4c** (B) at a concentration of 200 ppm.

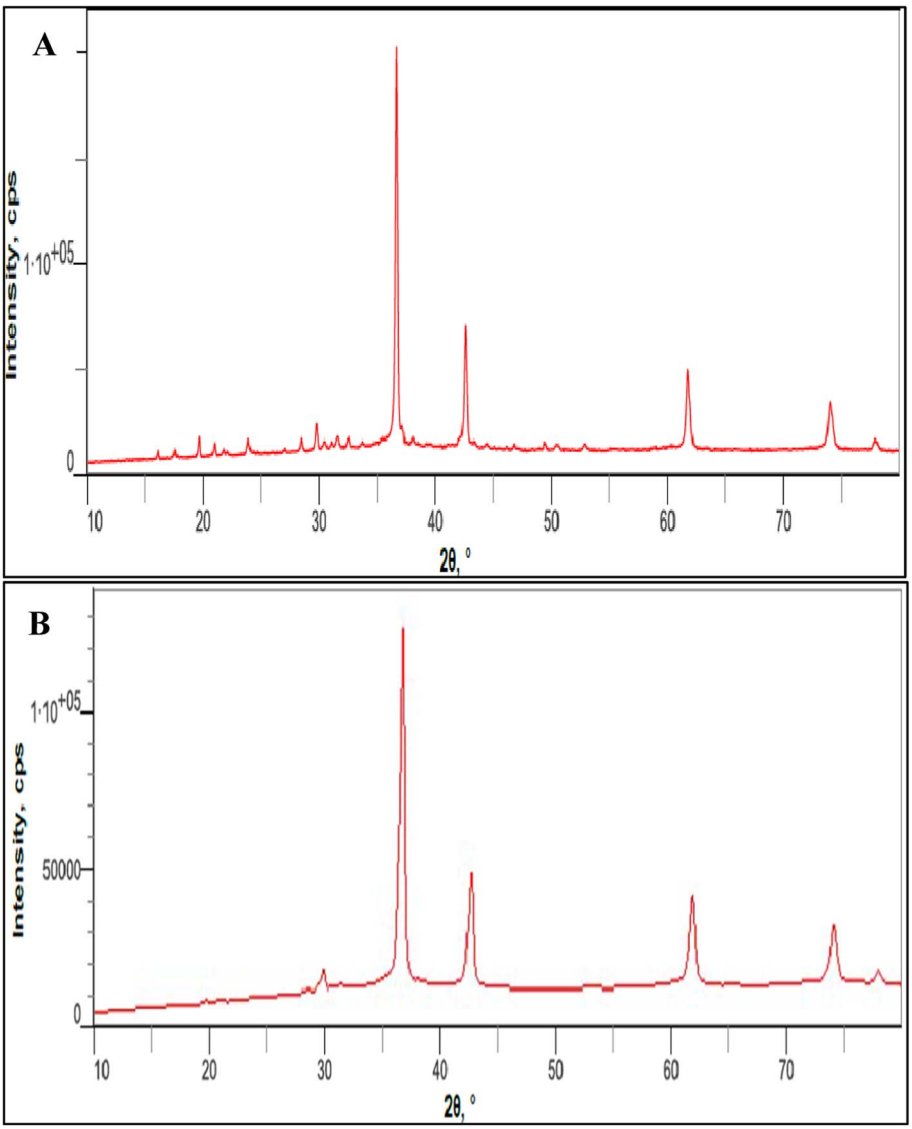

Fig. 7 Powder XRD patterns of the prepared Cu_2O NPs induced by GILBS **4a** (A) and **4c** (B) at a concentration of 200 ppm.

temperature, fine chemicals, and long time. It produces nanoparticles with relatively small sizes.

4 Conclusion

In this study, three new gemini ionic liquid-based surfactants GILBSs were synthesized and characterized. The polar head of these surfactants included the imidazolium cation with ethane-1,2-diyl as the spacer. Investigations into the surface properties and thermodynamic parameters of these compounds were extensively reported. In order to fabricate cuprous oxide nanoparticles, the prepared surfactants, **4a–c** were utilized in a variety of concentrations. Additionally, the impact of concentration on the morphology of the targeted nanoparticles was evaluated and to choose the optimal concentration among them, the size and shape of the nanoparticles were afterwards evaluated by XRD and TEM in each case. The size of the nanoparticles determined by TEM examinations and the ones estimated from XRD diffraction patterns are almost identical, and present indeed in the nano size with good size ranges even at very low concentrations.

Ethical statement

The study was conducted and approved according to the guidelines of the declaration of the ethical committee of the Faculty of Science, Benha University (No. 42 chm).

Conflicts of interest

All authors declare that they have no conflict of interest.

References

1 S. Marullo, C. Rizzo, N. T. Dintcheva, F. Giannici and F. D'Anna, Ionic liquids gels: Soft materials for

environmental remediation, *J. Colloid Interface Sci.*, 2018, **517**, 182.

2 Z. Zeng, B. S. Phillips, J.-C. Xiao and J. n. M. Shreeve, Polyfluoroalkyl, Polyethylene Glycol, 1,4-Bismethylenebenzene, or 1,4-Bismethylene-2,3,5,6-Tetrafluorobenzene Bridged Functionalized Dicationic Ionic Liquids: Synthesis and Properties as High Temperature Lubricants, *Chem. Mater.*, 2008, **20**, 2719.

3 Y. Cao, J. Wu, J. Zhang, H. Li, Y. Zhang and J. He, Room temperature ionic liquids (RTILs): A new and versatile platform for cellulose processing and derivatization, *Chem. Eng. J.*, 2009, **147**, 13.

4 S. Sasi, M. P. Rayaroth, C. T. Aravindakumar and U. K. Aravind, Identification of surfactants and its correlation with physicochemical parameters at the confluence region of Vembanad Lake in India, *Environ. Sci. Pollut. Res. Int.*, 2018, **25**, 20527.

5 M. Anouti, J. Jones, A. Boisset, J. Jacquemin, M. Caillon-Caravanier and D. Lemordant, Aggregation behavior in water of new imidazolium and pyrrolidinium alkycarboxylates protic ionic liquids, *J. Colloid Interface Sci.*, 2009, **340**, 104.

6 N. Cheng, X. Ma, X. Sheng, T. Wang, R. Wang, J. Jiao and L. Yu, Aggregation behavior of anionic surface active ionic liquids with double hydrocarbon chains in aqueous solution: Experimental and theoretical investigations, *Colloids Surf., A*, 2014, **453**, 53.

7 M. Ao and D. Kim, Aggregation Behavior of Aqueous Solutions of 1-Dodecyl-3-methylimidazolium Salts with Different Halide Anions, *J. Chem. Eng. Data*, 2013, **58**, 1529.

8 T. Singh and A. Kumar, Aggregation Behavior of Ionic Liquids in Aqueous Solutions: Effect of Alkyl Chain Length, Cations, and Anions, *J. Phys. Chem. B*, 2007, **111**, 7843.

9 B. Dong, X. Zhao, L. Zheng, J. Zhang, N. Li and T. Inoue, Aggregation behavior of long-chain imidazolium ionic liquids in aqueous solution: Micellization and characterization of micelle microenvironment, *Colloids Surf., A*, 2008, **317**, 666.

10 M. A. Rather, G. M. Rather, S. A. Pandit, S. A. Bhat and M. A. Bhat, Determination of cmc of imidazolium based surface active ionic liquids through probe-less UV-vis spectrophotometry, *Talanta*, 2015, **131**, 55.

11 N. V. Sastry, N. M. Vaghela and V. K. Aswal, Effect of alkyl chain length and head group on surface active and aggregation behavior of ionic liquids in water, *Fluid Phase Equilib.*, 2012, **327**, 22.

12 T. Singh, K. S. Rao and A. Kumar, Effect of ethylene glycol and its derivatives on the aggregation behavior of an ionic liquid 1-butyl-3-methyl imidazolium octylsulfate in aqueous medium, *J. Phys. Chem. B*, 2012, **116**, 1612.

13 T. Inoue, H. Ebina, B. Dong and L. Zheng, Electrical conductivity study on micelle formation of long-chain imidazolium ionic liquids in aqueous solution, *J. Colloid Interface Sci.*, 2007, **314**, 236.

14 A. Modaressi, H. Sifaoui, M. Mielcarz, U. Domańska and M. Rogalski, Influence of the molecular structure on the aggregation of imidazolium ionic liquids in aqueous solutions, *Colloids Surf., A*, 2007, **302**, 181.

15 O. A. El Seoud, N. Keppeler, N. I. Malek and P. D. Galgano, Ionic Liquid-Based Surfactants: Recent Advances in Their Syntheses, Solution Properties, and Applications, *Polymers*, 2021, **13**, 1100.

16 N. I. Malek, Z. S. Vaid, U. U. More and O. A. El Seoud, Ionic-liquid-based surfactants with unsaturated head group: synthesis and micellar properties of 1-(n-alkyl)-3-vinylimidazolium bromides, *Colloid Polym. Sci.*, 2015, **293**, 3213.

17 R. Vanyúr, L. Biczók and Z. Miskolczy, Micelle formation of 1-alkyl-3-methylimidazolium bromide ionic liquids in aqueous solution, *Colloids Surf., A*, 2007, **299**, 256.

18 F. Geng, J. Liu, L. Zheng, L. Yu, Z. Li, G. Li and C. Tung, Micelle Formation of Long-Chain Imidazolium Ionic Liquids in Aqueous Solution Measured by Isothermal Titration Microcalorimetry, *J. Chem. Eng. Data*, 2010, **55**, 147.

19 M. Blesic, A. n. Lopes, E. Melo, Z. Petrovski, N. V. Plechkova, J. N. C. Lopes, K. R. Seddon and L. s. P. N. Rebelo, On the Self-Aggregation and Fluorescence Quenching Aptitude of Surfactant Ionic Liquids, *J. Phys. Chem. B*, 2008, **112**, 8645.

20 A. Cornellas, L. Perez, F. Comelles, I. Ribosa, A. Manresa and M. T. Garcia, Self-aggregation and antimicrobial activity of imidazolium and pyridinium based ionic liquids in aqueous solution, *J. Colloid Interface Sci.*, 2011, **355**, 164.

21 M. Blesic, M. H. Marques, N. V. Plechkova, K. R. Seddon, L. P. N. Rebelo and A. n. Lopes, Self-aggregation of ionic liquids: micelle formation in aqueous solution, *Green Chem.*, 2007, **9**, 481.

22 H. Wang, J. Wang, S. Zhang and X. Xuan, Structural Effects of Anions and Cations on the Aggregation Behavior of Ionic Liquids in Aqueous Solutions, *J. Phys. Chem. B*, 2008, **112**, 16682.

23 X. Wang, J. Liu, L. Yu, J. Jiao, R. Wang and L. Sun, Surface adsorption and micelle formation of imidazolium-based zwitterionic surface active ionic liquids in aqueous solution, *J. Colloid Interface Sci.*, 2013, **391**, 103.

24 B. Dong, N. Li, L. Zheng, L. Yu and T. Inouen, Surface Adsorption and Micelle Formation of Surface Active Ionic Liquids in Aqueous Solution, *Langmuir*, 2007, **23**, 4178.

25 O. A. El Seoud, P. A. Pires, T. Abdel-Moghny and E. L. Bastos, Synthesis and micellar properties of surface-active ionic liquids: 1-alkyl-3-methylimidazolium chlorides, *J. Colloid Interface Sci.*, 2007, **313**, 296.

26 M. K. Ali, R. M. Moshikur, R. Wakabayashi, Y. Tahara, M. Moniruzzaman, N. Kamiya and M. Goto, Synthesis and characterization of choline-fatty-acid-based ionic liquids: A new biocompatible surfactant, *J. Colloid Interface Sci.*, 2019, **551**, 72.

27 T. J. Trivedi, K. S. Rao, T. Singh, S. K. Mandal, N. Sutradhar, A. B. Panda and A. Kumar, Task-specific, biodegradable amino acid ionic liquid surfactants, *ChemSusChem*, 2011, **4**, 604.

28 P. S. Gehlot, A. Kulshrestha, P. Bharmoria, K. Damarla, K. Chokshi and A. Kumar, Surface-Active Ionic Liquid Cholinium Dodecylbenzenesulfonate: Self-Assembling

Behavior and Interaction with Cellulase, *ACS Omega*, 2017, **2**, 7451.

29 M. U. H. Shah, M. Sivapragasam, M. Moniruzzaman, M. M. R. Talukder, S. B. Yusup and M. Goto, Aggregation behavior and antimicrobial activity of a micellar system of binary ionic liquids, *J. Mol. Liq.*, 2018, **266**, 568.

30 K. S. Rao, P. S. Gehlot, T. J. Trivedi and A. Kumar, Self-assembly of new surface active ionic liquids based on Aerosol-OT in aqueous media, *J. Colloid Interface Sci.*, 2014, **428**, 267.

31 M. J. Rosen and D. J. Tracy, Gemini Surfactants, *J. Surfactants Deterg.*, 1998, **1**, 547.

32 R. Zana, Alkanediyl-alpha,omega-bis(dimethylalkylammonium bromide) surfactants 10. Behavior in aqueous solution at concentrations below the critical micellization concentration: an electrical conductivity study, *J. Colloid Interface Sci.*, 2002, **246**, 182.

33 F. M. Menger and C. A. Littau, Gemini Surfactants: A New Class of Self-Assembling Molecules, *J. Am. Chem. Soc.*, 1993, **115**, 10083.

34 J. r. m. Gaucheron, T. Wong, K. F. Wong, N. Maurer and P. R. Cullis, Synthesis and Properties of Novel Tetraalkyl Cationic Lipids, *Bioconjugate Chem.*, 2002, **13**, 671–675.

35 E. Fisicaro, C. Compari, E. Duce, G. Donofrio, B. Rozycka-Roszak and E. Wozniak, Biologically active bisquaternary ammonium chlorides: physico-chemical properties of long chain amphiphiles and their evaluation as non-viral vectors for gene delivery, *Biochim. Biophys. Acta*, 2005, **1722**, 224.

36 S. M. Rajput, U. U. More, Z. S. Vaid, K. D. Prajapati and N. I. Malek, Impact of organic solvents on the micellization and interfacial behavior of ionic liquid based surfactants, *Colloids Surf., A*, 2016, **507**, 182.

37 S. M. Tawfik, Simple one step synthesis of gemini cationic surfactant-based ionic liquids: Physicochemical, surface properties and biological activity, *J. Mol. Liq.*, 2015, **209**, 320.

38 R. Goutham, P. Rohit, S. S. Vigneshwar, A. Swetha, J. Arun, K. P. Gopinath and A. Pugazhendhi, Ionic liquids in wastewater treatment: A review on pollutant removal and degradation, recovery of ionic liquids, economics and future perspectives, *J. Mol. Liq.*, 2022, **349**, 118150.

39 R. M. Moshikur, M. K. Ali, M. Moniruzzaman and M. Goto, Recent advances in surface-active ionic liquid-assisted self-assembly systems for drug delivery, *Curr. Opin. Colloid Interface Sci.*, 2021, **56**, 101515.

40 R. M. F. Bento, M. R. Almeida, P. Bharmoria, M. G. Freire and A. P. M. Tavares, Improvements in the enzymatic degradation of textile dyes using ionic-liquid-based surfactants, *Sep. Purif. Technol.*, 2020, **235**, 116191.

41 K. Qiao and Y. Zeng, Comparative study on two imidazolium-based ionic liquid surfactants as corrosion inhibitors for N80 steel in 15% hydrochloric acid solution, *Mater. Corros.*, 2020, **71**, 1913.

42 R. Bussamara, W. W. Melo, J. D. Scholten, P. Migowski, G. Marin, M. J. Zapata, G. Machado, S. R. Teixeira, M. A. Novak and J. Dupont, Controlled synthesis of Mn_3O_4 nanoparticles in ionic liquids, *Dalton Trans.*, 2013, **42**, 14473.

43 K.-S. Kim, D. Demberelnyamba and H. Lee, Size-Selective Synthesis of Gold and Platinum Nanoparticles Using Novel Thiol-Functionalized Ionic Liquids, *Langmuir*, 2004, **20**, 556.

44 O. Naderi, M. Nyman, M. Amiri and R. Sadeghi, Synthesis and characterization of silver nanoparticles in aqueous solutions of surface active imidazolium-based ionic liquids and traditional surfactants SDS and DTAB, *J. Mol. Liq.*, 2019, **273**, 645.

45 K. Schutte, H. Meyer, C. Gemel, J. Barthel, R. A. Fischer and C. Janiak, Synthesis of Cu, Zn and Cu/Zn brass alloy nanoparticles from metal amidinate precursors in ionic liquids or propylene carbonate with relevance to methanol synthesis, *Nanoscale*, 2014, **6**, 3116.

46 G. Singh, K. Komal, G. Singh, M. Kaur and T. S. Kang, A new sustainable approach towards preparation of sunlight active Ag/AgBr Janus nanoparticles using non-toxic surface active ionic liquid, *J. Mater. Chem. A*, 2019, **7**, 5185.

47 D. S. Jacob, L. Bitton, J. Grinblat, I. Felner, Y. Koltypin and A. Gedanken, Are Ionic Liquids Really a Boon for the Synthesis of Inorganic Materials? A General Method for the Fabrication of Nanosized Metal Fluorides, *Chem. Mater.*, 2006, **18**, 3162.

48 C. M. Lee, H. J. Jeong, S. T. Lim, M. H. Sohn and D. W. Kim, Synthesis of iron oxide nanoparticles with control over shape using imidazolium-based ionic liquids, *ACS Appl. Mater. Interfaces*, 2010, **2**, 756.

49 E. Redel, R. Thomann and C. Janiak, First Correlation of Nanoparticle Size-Dependent Formation with the Ionic Liquid Anion Molecular Volume, *Inorg. Chem.*, 2008, **47**, 14–16.

50 H. J. Ryu, L. Sanchez, H. A. Keul, A. Raj and M. R. Bockstaller, Imidazolium-based ionic liquids as efficient shape-regulating solvents for the synthesis of gold nanorods, *Angew. Chem., Int. Ed.*, 2008, **47**, 7639.

51 Y. Wang and H. Yang, Synthesis of iron oxide nanorods and nanocubes in an imidazolium ionic liquid, *Chem. Eng. J.*, 2009, **147**, 71.

52 Y. J. Zhu, W. W. Wang, R. J. Qi and X. L. Hu, Microwave-assisted synthesis of single-crystalline tellurium nanorods and nanowires in ionic liquids, *Angew. Chem., Int. Ed.*, 2004, **43**, 1410.

53 M. Abo-Riya, A. H. Tantawy and W. El-Dougdoug, Synthesis and evaluation of novel cationic gemini surfactants based on Guava crude fat as petroleum-collecting and dispersing agents, *J. Mol. Liq.*, 2016, **221**, 642.

54 S. Livi, J. Duchet-Rumeau, T. N. Pham and J. F. Gerard, Synthesis and physical properties of new surfactants based on ionic liquids: Improvement of thermal stability and mechanical behaviour of high density polyethylene nanocomposites, *J. Colloid Interface Sci.*, 2011, **354**, 555.

55 M. J. Schick and E. A. Beyer, Foaming Properties of Nonionic Detergents, *J. Am. Oil Chem. Soc.*, 1963, **40**, 66.

56 S. M. Alazrak, S. Awad, A. A. Khalil and W. El-Dougdoug, Synthesis and evaluation of new cationic polymeric

surfactant based on N-phthalimidomethyl methacrylate. Egypt, *J. Chem.*, 2021, **64**, 3861.

57 H. I. Mohamed, M. Z. Basyouni, A. A. Khalil, K. A. Hebash and A. H. Tantawy, Petroleum-dispersing and antimicrobial activity of newly synthesized polymeric surfactants tethering tetrachlorophthalimide moiety, *J. Iran. Chem. Soc.*, 2021, **18**, 265.

58 B. A. A. Bader, A. H. Tantawy, M. M. Azab and W. El-Dougdoug, Novel Synthesized Cationic Gemini Surfactants Bearing Amido Group and Their Application in Nanotechonoly, *Curr. Sci. Int.*, 2022, **11**, 184.

59 W. I. El-Dougdoug, A. S. Al-Gorair, A. Abou Elsaoud, H. Hawsawi, A. Elaraby, E. S. Mabrouk and M. Abdallah, Synthesis and assessment of Gemini cationic surfactants as inhibitors for corrosion of carbon steel in hydrochloric acid, *Green Chem. Lett. Rev.*, 2022, **15**, 796.

60 A. Abd-ElHamid, W. El-dougdoug, S. M. Syam, I. Aiad, S. M. Shaban and D.-H. Kim, Synthesis of gemini cationic surfactants-based pyridine Schiff base for steel corrosion and sulfate reducing bacteria mitigation, *J. Mol. Liq.*, 2023, **369**, 120890.

61 A. M. Badawi, M. A. S. Mohamed, M. Z. Mohamed and M. M. Khowdairy, Surface and antitumor activity of some novel metal-based cationic surfactants, *J. Cancer Res. Ther.*, 2007, **3**, 198.

62 N. A. Negm and S. M. Tawfik, Characterization, surface properties and biological activity of some synthesized anionic surfactants, *J. Ind. Eng. Chem.*, 2014, **20**, 4463.

63 C. Ren, F. Wang, Z. Zhang, H. Nie, N. Li and M. Cui, Synthesis, surface activity and aggregation behavior of Gemini imidazolium surfactants 1,3-bis(3-alkylimidazolium-1-yl) propane bromide, *Colloids Surf., A*, 2015, **467**, 1.

64 N. A. Negm, A. F. El-Farargy, S. M. Tawfik, A. M. Abdelnour, H. H. Hefni and M. M. Khowdiary, Synthesis, Surface and Thermodynamic Properties of Substituted Polytriethanolamine Nonionic Surfactants, *J. Surfactants Deterg.*, 2012, **16**, 333.

65 A. Mittiga, E. Salza, F. Sarto, M. Tucci and R. Vasanthi, Heterojunction solar cell with 2% efficiency based on a Cu_2O substrate, *Appl. Phys. Lett.*, 2006, **88**, 163502.

66 M. B. Gawande, A. Goswami, F. X. Felpin, T. Asefa, X. Huang, R. Silva, X. Zou, R. Zboril and R. S. Varma, Cu and Cu-Based Nanoparticles: Synthesis and Applications in Catalysis, *Chem. Rev.*, 2016, **116**, 3722.

67 J. C. Park, J. Kim, H. Kwon and H. Song, Gram-Scale Synthesis of Cu2O Nanocubes and Subsequent Oxidation to CuO Hollow Nanostructures for Lithium-Ion Battery Anode Materials, *Adv. Mater.*, 2009, **21**, 803.

68 L. Gou and C. J. Murphy, Solution-Phase Synthesis of Cu_2O Nanocubes, *Nano Lett.*, 2003, **3**, 231.

69 M. Salavati-Niasari and F. Davar, Synthesis of copper and copper(I) oxide nanoparticles by thermal decomposition of a new precursor, *Mater. Lett.*, 2009, **63**, 441.

70 R. V. Kumar, Y. Mastai, Y. Diamant and A. Gedanken, Sonochemical synthesis of amorphous Cu and nanocrystalline Cu2O embedded in a polyaniline matrix, *J. Mater. Chem.*, 2001, **11**, 1209.

71 X. M. Sun, X. Chen, Z. X. Deng and Y. D. Li, A CTAB-assisted hydrothermal orientation growth of ZnO nanorods, *Mater. Chem. Phys.*, 2002, **78**, 99.

72 M. Kooti and L. Matouri, Fabrication of Nanosized Cuprous Oxide Using Fehling's Solution, *Trans. F*, 2010, **17**, 73.

73 A.-L. Daltin, A. Addad and J.-P. Chopart, Potentiostatic deposition and characterization of cuprous oxide films and nanowires, *J. Cryst. Growth*, 2005, **282**, 414.

74 D. A. Firmansyah, T. Kim, S. Kim, K. Sullivan, M. R. Zachariah and D. Lee, Crystalline phase reduction of cuprous oxide (Cu2O) nanoparticles accompanied by a morphology change during ethanol-assisted spray pyrolysis, *Langmuir*, 2009, **25**, 7063.

75 Y. Sui, Y. Zeng, W. Zheng, B. Liu, B. Zou and H. Yang, Synthesis of polyhedron hollow structure Cu2O and their gas-sensing properties, *Sens. Actuators, B*, 2012, **171–172**, 135.

76 Y. Bai, T. Yang, Q. Gu, G. Cheng and R. Zheng, Shape control mechanism of cuprous oxide nanoparticles in aqueous colloidal solutions, *Powder Technol.*, 2012, **227**, 35.

77 M. H. Huang and C.-Y. Chiu, Achieving polyhedral nanocrystal growth with systematic shape control, *J. Mater. Chem. A*, 2013, **1**, 8081.